Gait & Posture 37 (2013) 264–268

Contents lists available at SciVerse ScienceDirect

Gait & Posture

journal homepage: www.elsevier.com/locate/gaitpost

Posterior tibial tendon dysfunction and flatfoot: Analysis with simulated walking

Kota Watanabe [a,b], Harold B. Kitaoka [a], Tadashi Fujii [a], Xavier Crevoisier [a], Lawrence J. Berglund [a], Kristin D. Zhao [a], Kenton R. Kaufman [a], Kai-Nan An [a,*]

[a] Department of Orthopedic Surgery, Mayo Clinic, Rochester, MN, USA
[b] Department of Orthopedic Surgery, Sapporo Medical University School of Medicine, Sapporo, Japan

ARTICLE INFO

Article history:
Received 11 October 2011
Received in revised form 16 July 2012
Accepted 21 July 2012

Keywords:
Flatfoot
Kinematics
Simulator
Cadaver
Gait simulation

ABSTRACT

Many biomechanical studies investigated pathology of flatfoot and effects of operations on flatfoot. The majority of cadaveric studies are limited to the quasistatic response to static joint loads. This study examined the unconstrained joint motion of the foot and ankle during stance phase utilizing a dynamic foot–ankle simulator in simulated stage 2 posterior tibial tendon dysfunction (PTTD). Muscle forces were applied on the extrinsic tendons of the foot using six servo-pneumatic cylinders to simulate their action. Vertical and fore-aft shear forces were applied and tibial advancement was performed with the servomotors. Three-dimensional movements of multiple bones of the foot were monitored with a magnetic tracking system. Twenty-two fresh-frozen lower extremities were studied in the intact condition, then following sectioning peritalar constraints to create a flatfoot and unloading the posterior tibial muscle force. Kinematics in the intact condition were consistent with gait analysis data for normals. There were altered kinematics in the flatfoot condition, particularly in coronal and transverse planes. Calcaneal eversion relative to the tibia averaged $11.1 \pm 2.8^\circ$ compared to $5.8 \pm 2.3^\circ$ in the normal condition. Calcaneal-tibial external rotation was significantly increased in flatfeet from mean of $2.3 \pm 1.7^\circ$ to $8.1 \pm 4.0^\circ$. There were also significant changes in metatarsal-tibial eversion and external rotation in the flatfoot condition. The simulated PTTD with flatfoot was consistent with previous data obtained in patients with PTTD. The use of a flatfoot model will enable more detailed study on the flatfoot condition and/or effect of surgical treatment.

1. Introduction

In recent years, there have been multiple reports related to posterior tibial tendon dysfunction (PTTD). PTTD is a common cause of acquired flatfoot deformity in adults; the condition may reach a prevalence of 10% in elderly women [1]. Most of the clinical investigations reported the effects of various operations to correct PTTD and flatfoot deformity, but *in vitro* and radiologic studies have also been published [2–5]. The optimum management of stage 2 PTTD [2] in which there is a mobile flatfoot has been a subject of debate for more than two decades. There are questions regarding the pathoanatomy of the deformity resulting from tendon dysfunction. A comprehensive understanding of the flatfoot malalignment will lead to more effective techniques for correcting it.

Previous investigators recognized the importance of defining the flatfoot and quantitating the degree of deformation [6]. Clinical measurements such as arch height have been used, but were not consistent between examiners [6]. Radiologic measurements of flatfoot have been performed in patients with PTTD [4,5]. Analysis of foot prints and ground reaction data in flatfeet have been reported [7]. Previous reports determined the contribution of various static elements in supporting the arch [8]. Others indicated that the posterior tibial tendon (PTT) plays a role in the dynamic support of the arch [3]. Most of these previous reports were *in vitro* studies with static loading of specimens. Recent gait analysis studies have revealed kinematics changes of the foot between normal and flatfoot [9–12]. *In vitro*, dynamic joint simulators have been developed recently for foot/ankle as well as other joints and applied for biomechanical studies of pathological situations of foot/ankle problems [13–19]. However, there have not been any publications, to our knowledge, detailing the three-dimensional kinematics of the flatfoot during simulated walking of the entire stance phase of gait.

We developed a dynamic foot–ankle simulator capable of recreating the stance phase of gait in cadaveric lower extremities [15]. It allows simulation of functional activities by allowing unconstrained motion of the foot and ankle while simultaneously applying time-histories of forces that affect the foot. A dynamic

* Corresponding author at: Mayo Clinic, 200 First Street SW, Rochester, MN 55905, USA. Tel.: +1 507 538 1717; fax: +1 507 284 5392.
E-mail address: an@mayo.edu (K.-N. An).

0966-6362/$ – see front matter © 2012 Elsevier B.V. All rights reserved.
http://dx.doi.org/10.1016/j.gaitpost.2012.07.015

simulator will be useful for improving our understanding of the mechanical behavior of the flatfoot compared to the normal foot. The purpose of the study was to examine unconstrained joint motion of the foot and ankle during stance phase in cadaveric lower extremities with simulated PTTD with flatfoot deformity utilizing a dynamic foot–ankle simulator.

2. Methods

Twenty-two fresh-frozen lower extremities were evaluated after gross visual screening for preexisting abnormalities of the foot. The mean age of the specimens was 78 years old (range, 47–95). Five were female, 17 male. Fourteen specimens were left feet and eight were right. The institutional research ethics committee reviewed and approved the study.

The custom simulator was able to subject cadaveric foot and ankle specimens to specified time-histories of normative ground reaction forces (GRF), and tendon loading based on physiological cross-sectional area (PCSA) and electromyography (EMG) data. Adjustments were made the initial muscle force profiles to match normal patterns of calcaneal-tibial angles and gross forefoot motion, while allowing totally unconstrained joint motions. The inputs were the forward tibial motion, fore-aft shear loading, tibial loading, and muscle loading. The outputs were measured foot reaction (force and center-of-pressure advancement) and joint kinematics. Since few biomechanical models were available for this hybrid (load and motion) control system, the tibial loading was prescribed to the normal vertical GRF profile as an approximation using a closed-loop servomotor so as to match the normal vertical GRF despite the disturbances from the muscle loading actuators. Ankle joint kinematics was controlled by muscle loading, which was initially targeted from the muscle gain, PCSA, and EMG data for each muscle group.

The leg specimen, amputated at the mid-tibial level, was potted in an acrylic plastic tube with polymethylmethacrylate cement, and fixed on the tendon loading unit (Fig. 1) [15]. The tendon-loading unit, consisting of six pneumatic cylinders, was connected through a linear ball screw to the servomotor tibial angle control unit, and through a hinge joint to the vertical loading unit. All the above units created a four-bar rocker configuration to control the angle of the loading unit or tibia relative to the ankle joint during the simulation. The vertical-loading unit, mounted on the frame, was connected to a linear slide powered by a linear ball screw and servomotor. This servomotor axis provided loading along the tibial axis by moving both the vertical loading unit and tendon loading unit onto the force plate. The sole of the foot contacted the custom-made force plate, which recorded the simulated vertical GRF. The bearing plate beneath the force plate allowed the relative forward translation of the foot and ankle and accommodated the anteroposterior shear force [20] by coupling the plate to another closed-loop servo axis. Most structures were built using non-metallic tubing or acrylic plastics, to minimize any interference with the magnetic tracking system.

The tibial angle control unit translated the tibial motion between 20° anterior and 40° posterior to vertical [21]. During testing, the tibial angle was monitored by a potentiometer. The tibial angle was used to determine the percentage of stance phase from the tibial angle history profile [21]. The estimated percent stance phase was used to prescribe the tendon and tibial loading [20,21]. The extrinsic muscles acting on or around the ankle were divided into six functional units: gastrocnemius-soleus, PTT, flexor hallucis longus-flexor digitorum longus, anterior tibial, extensor hallucis longus-extensor digitorum longus, and peroneus longus-peroneus brevis. A total of six pneumatic cylinders driven by servo-pneumatic valves were used to apply loads to the tendons. Sutures were attached to each tendon using a modified Krackow technique except for the Achilles tendon, which was sutured using a Leeds-Keio artificial ligament (Ellis Developments, Nottingham, UK) to sustain the comparable physiological loading. A uniaxial load cell was connected to each cylinder to monitor the load feedback signal to an IBM PC. A custom-written program (LabVIEW®, National Instruments, Austin, TX) was used for control and kinetic data acquisition. Tendon loads were estimated from PCSA and EMG data in the literature [20,22]. A linear EMG and force relationship was assumed [23,24]. An unknown muscle gain K and the corresponding cross sectional area (PCSAi) were multiplied by the relative EMG data (EMGi) to provide absolute forces to each cylinder ($Fi = K \times PCSAi \times EMGi$). To determine the unknown muscle gain or muscle stress, simulations were repeated until the gross foot–ankle kinematics matched reasonably well to the stance phase center-of-pressure and motion patterns, while the gain of the muscles was simultaneously adjusted. The applied vertical and fore-aft loads were reduced for the cadaver feet due to the limited suture strength and age of the specimens.

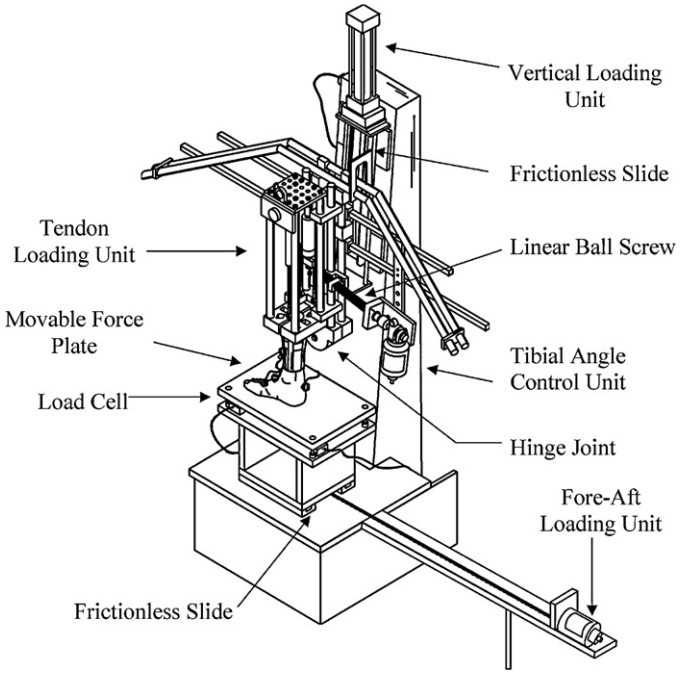

Fig. 1. Schematic drawing of the dynamic foot/ankle simulator.

Each specimen was cycled additional times through the entire stance phase to reduce the viscoelastic effect of soft tissues. The leg was then continuously moved from tibial flexion −20° (initial contact) to 40° flexion (pre-swing) while applying forces to the six muscle groups and subjecting it to the ground reaction force profiles. After testing the intact condition, a flatfoot condition was created by sectioning the peritalar soft tissue structures, including the spring ligament, long and short plantar ligaments, talocalcaneal interosseous ligament, medial talocalcaneal ligament, and tibionavicular portion of the superficial deltoid ligament. In order to simulate stage 2 PTTD and flatfoot, the posterior tibial muscle action was not simulated. A previous study [8] showed that flatfoot deformity occurred after these procedures, similar to that caused by stage 2 PTTD clinically. The applied vertical and fore-aft loads were not changed before and after the flatfoot model was created. Testing was performed three times for each condition and the average result was used for analysis.

Three-dimensional movements of the calcaneus and first metatarsus relative to the tibia were obtained with a magnetic tracking system (3Space Tracker System, Polhemus, Colchester, VT) [25,26]. The electromagnetic transmitter was fixed to the loading frame. Sensors were rigidly fixed to the anteromedial tibial diaphysis at the junction of the middle and distal thirds, posterolateral calcaneal body, and diaphysis of the dorsal-medial first metatarsal with acrylic mounting posts [26]. The relative angular motion between bones (calcaneal-tibial and first metatarsal-tibial) was expressed in terms of Eulerian angle description [25,26]. Bone positions were described relative to the previously described coordinate system [26]. The x-axis was oriented proximal-distal, the y-axis was oriented medial-lateral, and the z-axis was oriented anterior-posterior. The x-axis was along the tibial shaft through the ankle center, the z-axis was parallel to the projection of a line connecting the center of the heel and the second metatarsal on a plane perpendicular to the x-axis passing through the ankle center, and the y-axis was the product of the x- and z-axes following the right-hand rule passing through the ankle center. The three axes were also used to define the perpendicular planes: coronal (x–y plane), sagittal (x–z plane), and transverse (y–z plane). Motion was defined as inversion and eversion in the coronal plane, dorsiflexion and plantarflexion in the sagittal plane, and internal rotation and external rotation in the transverse plane.

Statistical analysis was performed with a paired t-test, comparing the bony positions in the intact and flatfoot conditions. The level of significance was set at $p < 0.05$.

3. Results

All the results of angular motions of the calcaneus and the first metatarsal relative to the tibia are presented over an entire stance phase that started with heel strike and ended with toe-off (Fig. 2). Angular movement patterns were consistent across all specimens. In the sagittal plane, the forefoot contacted with the force plate at about 10% stance phase. Maximum dorsiflexion was observed at about 80% stance phase. Then rapid plantarflexion occurred until maximum plantarflexion at toe-off. In the coronal plane, the hindfoot (calcaneal-tibial) and forefoot (metatarsal-tibial) moved from an initial inversion at heel strike to eversion. Maximum eversion occurred at a late phase of stance, prior to heel rise. Then the foot progressively inverted until toe-off. In the transverse plane, the hindfoot and forefoot moved from an initial internal rotation to external rotation. At mid-stance the foot reversed and began to internal rotate until toe-off.